Finite-Fault Modeling of Strong Ground Motion from the 2010 M_w 7.0 Haiti Earthquake

G.P. Mavroeidis & C.M. Scotti
The Catholic University of America, U.S.A.

A.S. Papageorgiou
University of Patras, Greece

SUMMARY:
At 21:53:10 UTC, on 12 January 2010, the small island nation of Haiti was devastated by an M_w 7.0 earthquake. Due to the socioeconomic environment in Haiti, no seismic recording stations were operating in the source region at the time of the earthquake. The lack of strong motion instruments has hindered the direct estimation of the amplitude, duration and frequency content of the ground shaking caused by the seismic event. In this study, synthetic broadband strong ground motions are generated in the vicinity of the 2010 Haiti earthquake. The low-frequency components of the synthetic ground motions are simulated using the discrete wavenumber representation method and the generalized transmission and reflection coefficient technique. The high-frequency ground motion components are generated using the specific barrier model. The two independently derived ground motion components are properly combined to generate broadband ground motion time histories and response spectra for the city of Port-au-Prince and for other sites in the vicinity of the earthquake.

Keywords: Haiti earthquake, synthetic ground motion, deterministic modeling, stochastic modeling

1. INTRODUCTION

At 21:53:10 UTC, on 12 January 2010, the small island nation of Haiti was devastated by an M_w 7.0 earthquake. The earthquake's hypocenter was located at (18.44°N, 72.57°W), according to the National Earthquake Information Center (NEIC) of the U.S. Geological Survey (USGS), and at depth of 13 km, just 25 km W-SW of the capital city of Port-au-Prince. It was originally assumed that the rupture occurred on the well-documented left-lateral strike-slip fault system in the vicinity of the earthquake known as the Enriquillo-Plantain Garden Fault (EPGF). However, further studies revealed a more complex nature to this seismic event as explained in a subsequent section.

The Haiti earthquake is considered one of the most destructive seismic events and one of the largest humanitarian catastrophes in recorded history. More than 220,000 people lost their lives, 310,000 people suffered often devastating injuries, and over 1.2 million people were left homeless. The earthquake also took a heavy toll on the infrastructure and buildings in the area, almost all of which were designed and constructed with no considerations for seismic loads. A detailed description of the observed structural and geotechnical damage in the Port-au-Prince region and other rural areas and towns to the west has been provided in several field reconnaissance reports (e.g., Eberhard *et al.*, 2010; Rathje *et al.*, 2010). The increased vulnerability of Haiti's infrastructure may be attributed to several factors, including the absence of seismic building codes, uncontrolled construction practices, and poor building material quality.

Due to the socioeconomic environment in Haiti, no seismic recording stations were operating in the source region at the time of the earthquake. This lack of strong motion instruments has hindered the direct estimation of the intensity, duration and frequency content of the ground shaking caused by this seismic event. In this study, synthetic broadband strong ground motions are generated in the vicinity of the earthquake by using a hybrid simulation approach that is based on physical models of the

extended seismic source. The low-frequency components of the synthetic ground motions are simulated using the slip model proposed by Hayes *et al*. (2010). The computations are carried out using the discrete wavenumber representation method (Bouchon and Aki, 1977; Bouchon, 1979) and the generalized transmission and reflection coefficient technique (Luco and Apsel, 1983). In addition, a layered crustal model is considered to account for a more realistic propagation of the seismic wavefield through the medium. The high-frequency ground motion components are generated using the specific barrier model (Papageorgiou and Aki, 1983a,b). The two independently derived ground motion components are properly combined to generate broadband ground motion time histories and response spectra for the city of Port-au-Prince and for other sites in the vicinity of the earthquake. These simulation results have the potential to facilitate the development of a relationship between ground motion characteristics and observable damage due to the 2010 Haiti earthquake, and contribute to the development of safer seismic design practices in Haiti in the future.

2. EARTHQUAKE EVENT

2.1. Tectonic setting and historical earthquakes

Haiti occupies the western end of the island of Hispaniola, located in the NE Caribbean between Puerto Rico to the east and Cuba and Jamaica to the west. The island of Hispaniola lies on the northern boundary of the Caribbean plate and was formed as a result of the seismic activity along this boundary with the North American plate (Fig. 1). The boundary between the two tectonic plates is defined by a zone where several fault systems have been identified and is characterized by a left-lateral strike-slip motion which accommodates a slip of approximately 20 mm per year (Manaker *et al*., 2008). The southern peninsula of Haiti is bisected by the Enriquillo-Plantain Garden Fault (EPGF) which runs east-west bordering the northern edge of the Caribbean tectonic plate (Fig. 1). EPGF is characterized by an average slip of approximately 8 mm per year (Manaker *et al*., 2008). The remaining 12 mm per year of the Caribbean plate's eastward motion is being accommodated primarily by the Septentrional Fault (SF), a parallel fault system in northern Hispaniola (Manaker *et al*., 2008).

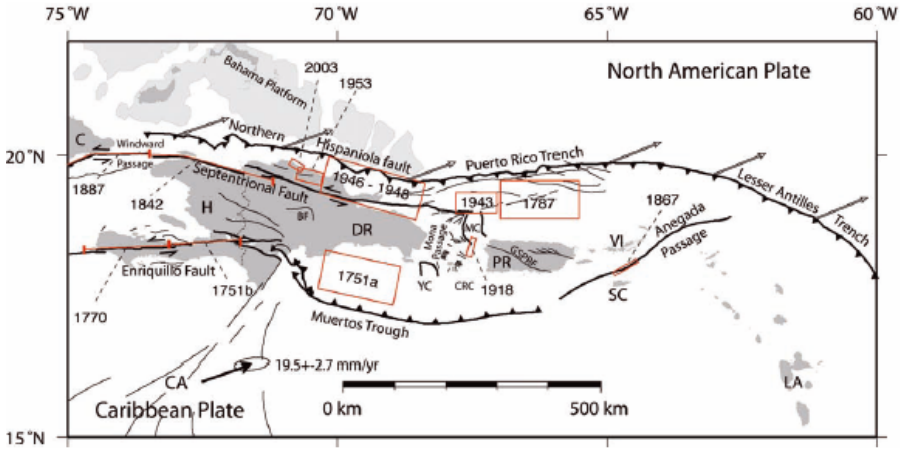

Figure 1. Major features of NE Caribbean, including regional faults and large earthquakes since 1564 (from Manaker *et al*., 2008).

2.2. Seismological observations and surface deformation

Both the Global Centroid Moment Tensor solution and inversions performed by USGS NEIC for the mainshock of 2010 Haiti earthquake indicated slip on a steeply dipping left-lateral strike-slip fault with a modest thrust component (i.e., strike ϕ = 246-251°, dip δ = 70-74°, rake λ = 22-28°, and seismic moment M_0 = 4.4-4.7 x 10^{19} N.m). The earthquake was initially presumed to have occurred on the well-documented EPGF which fits these parameters. However, as was pointed out by Nettles and

Hjorleifsdottir (2010) who studied the aftershock sequence of the 2010 Haiti earthquake, the most surprising result of their analysis was the dominance of reverse faulting mechanisms in the aftershock sequence, hinting at the existence of a separate reverse fault adjacent to the EPGF.

Field reconnaissance investigations (e.g., Eberhard *et al*., 2010; Rathje *et al*., 2010) failed to find any evidence of surface faulting along the EPGF, questioning its direct association with the 2010 Haiti earthquake. Furthermore, observations of coastal deformation showed that the fault rupture uplifted a broad region (~8 km in width) centered north of the EPGF. Given that such uplift over a broad region is not expected from a strike-slip earthquake, it was suggested that the fault rupture may have occurred on a steeply dipping blind or buried oblique-slip fault located north of the EPGF (Rathje *et al*., 2010). Finally, the palaeoseismic study by Prentice *et al.* (2010) revealed that no accumulated strain was released on the EPGF in the 2010 Haiti earthquake, confirming that the EPGF remains a significant seismic hazard for Port-au-Prince and raising serious questions about the tectonics of the region.

2.3. Faulting model

Calais *et al*. (2010) investigated the fault rupture process of the 2010 Haiti earthquake and attributed the rupture to a single north-dipping blind thrust fault. The distribution of slip on the causative fault plane was calculated based on a joint inversion of global positioning system (GPS) and interferometric synthetic aperture radar (InSAR) measurements of ground motion. Using InSAR data, Hashimoto *et al*. (2010) also demonstrated that the surface deformation caused by the 2010 Haiti earthquake was not consistent with present topography and determined the distribution of slip on a single blind fault dipping northward, with large thrust components.

Hayes *et al*. (2010) inferred the spatial and temporal slip distribution associated with the 2010 Haiti earthquake by combining seismological observations, geologic field data, and space geodetic measurements. A simulated-annealing algorithm was used to search for the optimal combination of slip, rake, rise time and rupture velocity to best fit the observed patterns resulting from the event. The proposed model consists of three idealized fault planes, labeled *A*, *B*, and *C* in Fig. 2. Faults *B* and *C* have been inferred to satisfy geodetic changes resulting from the earthquake, while Fault *A* is consistent with seismological parameters of the mainshock. The faulting model proposed by Hayes *et al*. (2010) is used in the present study to generate broadband ground motion time histories and response spectra for the city of Port-au-Prince and other sites in the vicinity of the earthquake. Fig. 3 shows the magnitude and direction of slip on Faults *A*, *B*, and *C*. At each subfault, the slip displacement is represented by a two-dimensional vector whose length is proportional to the average slip on that subfault and whose orientation is consistent with the rake angle.

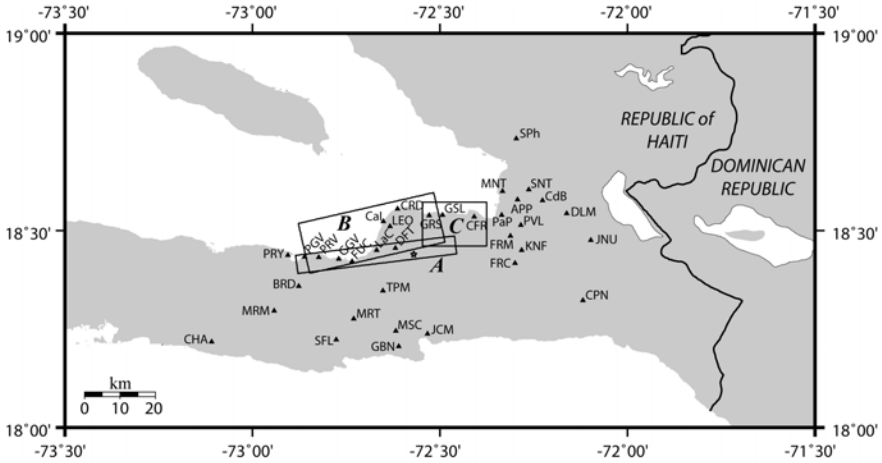

Figure 2. Map view of the 2010 Haiti earthquake, showing the location of the epicenter, the projection of the idealized fault models *A*, *B* and *C* inferred by Hayes *et al*. (2010) on the earth's surface, and sites selected for the ground motion simulations.

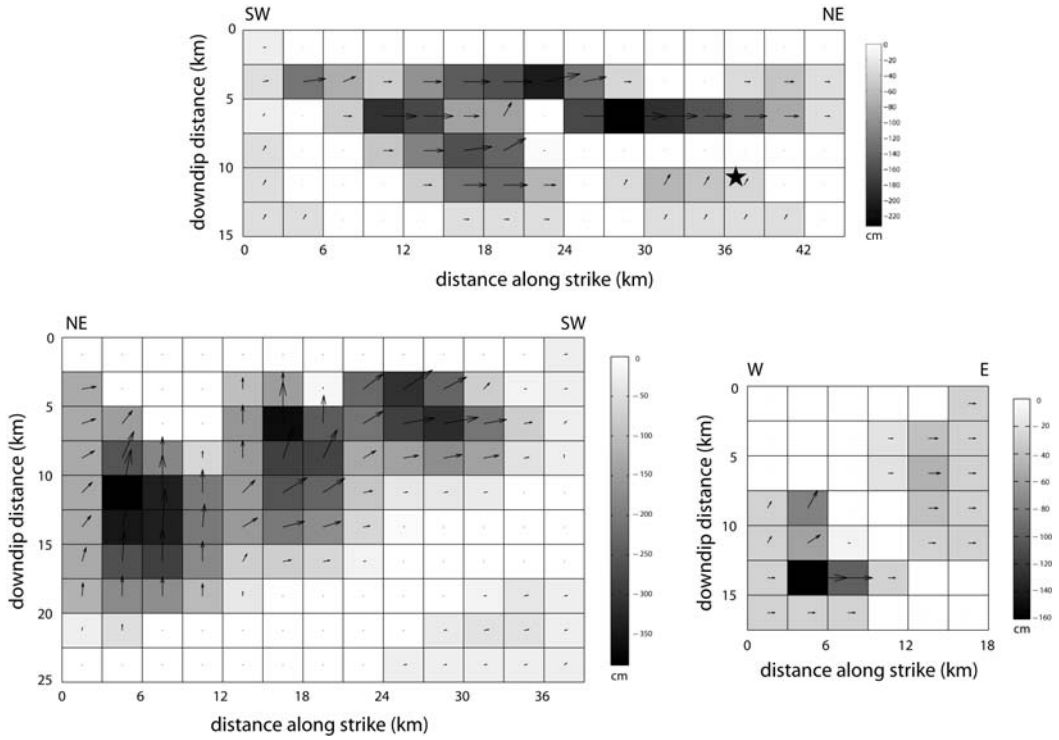

Figure 3. Tomographic images of the fault slip for Fault *A* (top), Fault *B* (bottom left) and Fault *C* (bottom right) of the 2010 Haiti earthquake inferred by Hayes *et al*. (2010).

Fault *A* is a 70° south-dipping fault similar in orientation to the EPGF, but may in fact be a parallel unidentified fault. This fault plane is 45 km long and 15 km wide, and has a strike angle of 83°. The upper-edge of the fault is located 0.2 km below the earth's surface. The fault experienced a predominantly left-lateral strike slip, occurring primarily at depths below 2.5 km, which explains the lack of surface deformation consistent with a strike-slip rupture. The fault has been discretized into 90 subfaults, each having a length of 3 km in the strike direction and 2.5 km in the dip direction. The maximum slip value on Fault *A* was 2.3 m. This fault contributed approximately 22% to the total seismic moment of the 2010 Haiti earthquake. The rise time was highly variable ranging from 0.6 to 7.8 s. According to Hayes *et al*. (2010), the hypocenter of the 2010 earthquake was located on Fault *A* at a depth of approximately 11 km. The rupture propagated bilaterally across the fault plane in roughly concentric circles, triggering ruptures on Faults *B* and *C*.

Fault *B*, also referred to as the Leogane fault, is a 55° north-dipping fault located just to the north of Fault *A*. This is a blind thrust fault that accounts for most of the coastal uplift in the region and the broad subsidence trough observed in the southern mountains. The fault has a strike of 257° and an upper edge that is approximately 4.4 km deep. It extends for 39 km in the strike direction and 25 km in the dip direction. The fault has been discretized into 130 subfaults, each having a dimension of 3 km in strike and 2.5 km in dip. Most of the slip occurring on the eastern portion of the fault was characterized by a dip-slip thrusting mechanism, while the western portion of the fault was characterized by right-lateral strike-slip motion. The maximum value of slip was approximately 3.9 m. This fault is credited with 73% of the seismic moment released during the earthquake. The rise time was highly variable ranging from 0.6 to 7.8 s. The rupture for Fault *B* started at the upper edge of the fault, roughly 6 km from the eastern most edge, and propagated downward along the fault.

Fault *C* is a small 45° south-dipping fault located to the east of Faults *A* and *B*. It was considered in the inversion in order to account for a patch of eastward surface movement that did not coincide with the overall left-lateral displacement of Fault *A*. Fault *C* has a strike of approximately 90° and an upper edge located 0.6 km below the surface of the earth. This fault is 18 km long and 17.5 km wide, and has

been discretized into 42 equally sized subfaults measuring 3 km in the strike direction and 2.5 in the dip direction. The maximum slip on Fault *C* was 1.6 m and was concentrated in the lower left and upper right portions of the fault. Fault *C* contributed approximately 5% to the total seismic moment of the 2010 Haiti earthquake and therefore affected only sites located in the immediate vicinity of this fault. The rise time was highly variable ranging from 0.6 to 7.8 s. The rupture for Fault *C* was initiated on the lower left edge of the fault plane, approximately 1.9 s after origination of rupture at the hypocenter, and propagated to the east along the fault.

3. CRUSTAL MODEL

The region in which the 2010 Haiti earthquake occurred has not been studied extensively for its crustal characteristics. A similarity between the crust in Haiti and the well-documented crust in the nearby island of Jamaica has been considered in the present study. Wiggins-Grandison (2004) used earthquake data recorded by the Jamaica Seismograph Network to obtain a one-dimensional layered crustal model for the island of Jamaica. The derived compressional and shear wave velocities are consistent with velocities reported elsewhere in the Caribbean as determined by geophysical exploration, indicating that crustal profiles around the region are similar. Therefore, it was assumed that the crustal model proposed by Wiggins-Grandison (2004) also applies to Haiti because of the close physical proximity of the two islands.

4. SIMULATION OF BROADBAND STRONG GROUND MOTION

The synthetic broadband ground motions for the 2010 Haiti earthquake are generated using a hybrid procedure that combines deterministic modeling at low frequencies with stochastic modeling at high frequencies. Using the discrete wavenumber representation method (Bouchon and Aki, 1977; Bouchon, 1979), the low-frequency ground motions are computed for each of the three faults inferred by Hayes *et al*. (2010), as well as for the overall seismic event. Similarly, using the specific barrier model (Papageorgiou and Aki, 1983a,b), the high-frequency ground motions are computed for each of the three faults, as well as for the overall event. Finally, the two independently derived components of ground motion are properly combined to provide broadband ground motion time histories and elastic response spectra for sites located in the vicinity of the earthquake.

4.1. Low-frequency ground motion simulation

The computation of the low-frequency ground motion is carried out using the discrete wavenumber representation method (Bouchon and Aki, 1977; Bouchon, 1979). The fault fracture is modeled as an ensemble of extended dislocation sources with rupture properties (e.g., slip, rise time, rupture velocity) consistent with the faulting model proposed by Hayes *et al*. (2010). The time dependence of slip at a given point on the fault is represented by a ramp function with spatially varying rise time. The generalized transmission and reflection coefficient technique (Luco and Apsel, 1983) is utilized for the propagation of the low-frequency wavefield through the one-dimensional layered crustal model proposed by Wiggins-Grandison (2004).

The low-frequency ground motion time histories are generated for 35 sites selected to coincide with the region of Port-au-Prince and other rural areas and towns surrounding the causative faults. Fig. 2 illustrates a location map of south-central Haiti, along with the relative locations of the 35 sites. Fig. 4 shows time histories of the low-frequency ($0< f <2.5$ Hz) velocity and displacement components for the cities of Port-au-Prince (PaP), Leogane (LEO) and Port Royal (PRY) over a time window of 70 s. The time series are presented with respect to an absolute time scale whose origin coincides with the nucleation of rupture at the hypocenter on Fault *A*. The horizontal components are oriented along the North-South (N-S) and East-West (E-W) directions. The directions pointing north, east and downwards define the positive sign convention of the synthetic ground motion time series.

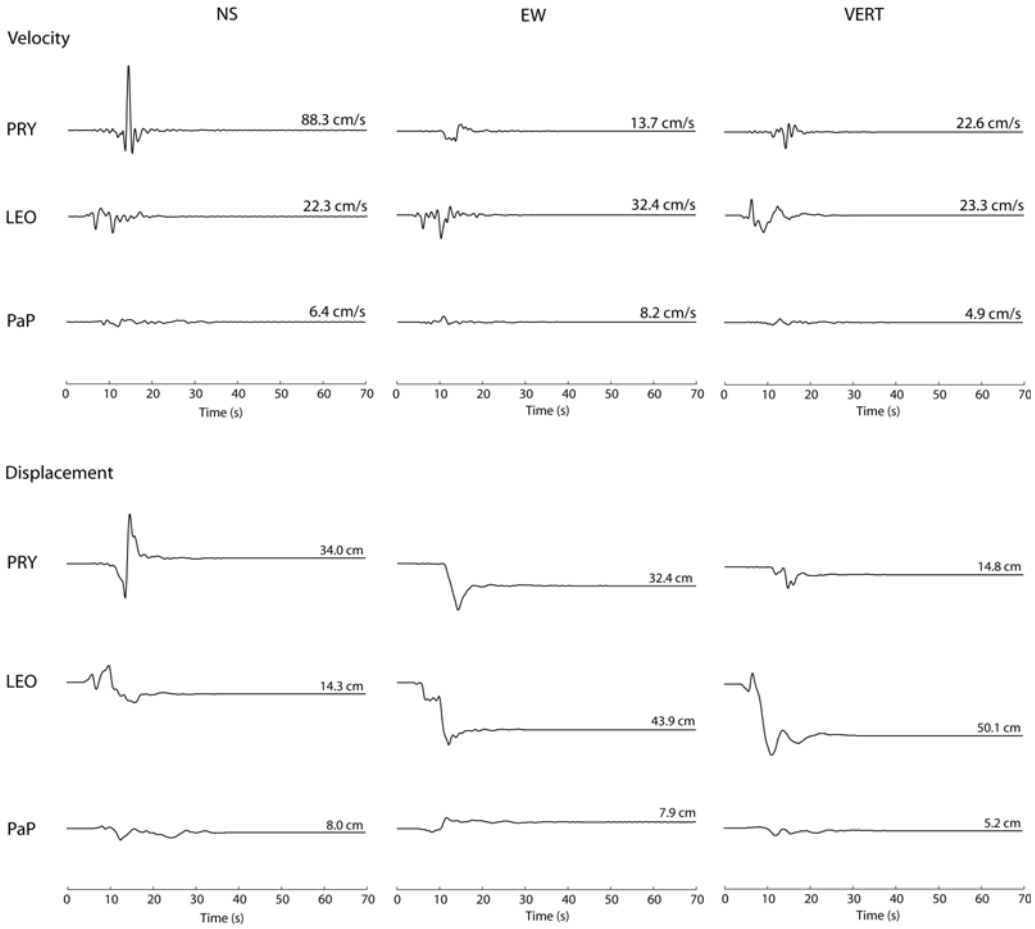

Figure 4. Synthetic low-frequency velocity and displacement time histories for selected sites of the 2010 Haiti earthquake. All components are plotted to the same amplitude scale.

4.2. High-frequency ground motion simulation

The computation of the high-frequency ground motion is carried out using the specific barrier model (SBM) (Papageorgiou and Aki, 1983a,b; Papageorgiou, 2003). This is a physical model of the seismic source that applies both in the "near-field" and "far-field" regions, allowing for consistent ground motion simulations over a wide frequency range and for all distances of engineering interest. In the SBM, the fault is visualized as an ensemble of non-overlapping circular subevents of equal diameter that cover a rectangular fault. As the rupture front sweeps the fault plane with a sweeping velocity, a local stress drop occurs on each subevent. The subevent rupture starts from its center and spreads radially outward with a constant spreading velocity until it is arrested by the barriers. It should be noted that the SBM is based on a finite-fault model of the extended seismic source that provides a clear and unambiguous way as to how to distribute the available seismic moment of the simulated event on the fault plane. This is a necessary requirement for synthesizing earthquake ground motions in the immediate vicinity of an extended seismic source.

The SBM is particularly simple in application due to the small number of physically well-defined input parameters. The scaling of these parameters with earthquake magnitude has been established in previous studies (Papageorgiou and Aki, 1983a; Papageorgiou, 1988). The SBM has been calibrated to shallow crustal earthquakes of three different tectonic regions: interplate, intraplate and extensional regimes (Halldorsson and Papageorgiou, 2005). Given an earthquake magnitude and the tectonic region, the interdependence of other source parameters on the local stress drop and the barrier interval allows the causative earthquake fault to be constructed. The calibrated SBM is used in the present

study to simulate the high-frequency ground motion in the vicinity of the 2010 Haiti earthquake.

Since all sites of interest for the 2010 Haiti earthquake are considered to be in the "near field" of the ruptured fault, it is necessary to simulate time histories for each individual subevent of the SBM using the stochastic method, rather than for the entire seismic event as an aggregate of subevents. As explained by Halldorsson *et al*. (2011), the subevent time histories are subsequently summed up at the site, appropriately lagged in time accounting for the time it takes the sweeping rupture front to reach the subevent and for the travel time of the seismic radiation from the subevent to the site. The high-frequency time histories simulated in this manner account for the directivity effects that the fault geometry and rupture progression have on the high-frequency strong motion expected at the given site.

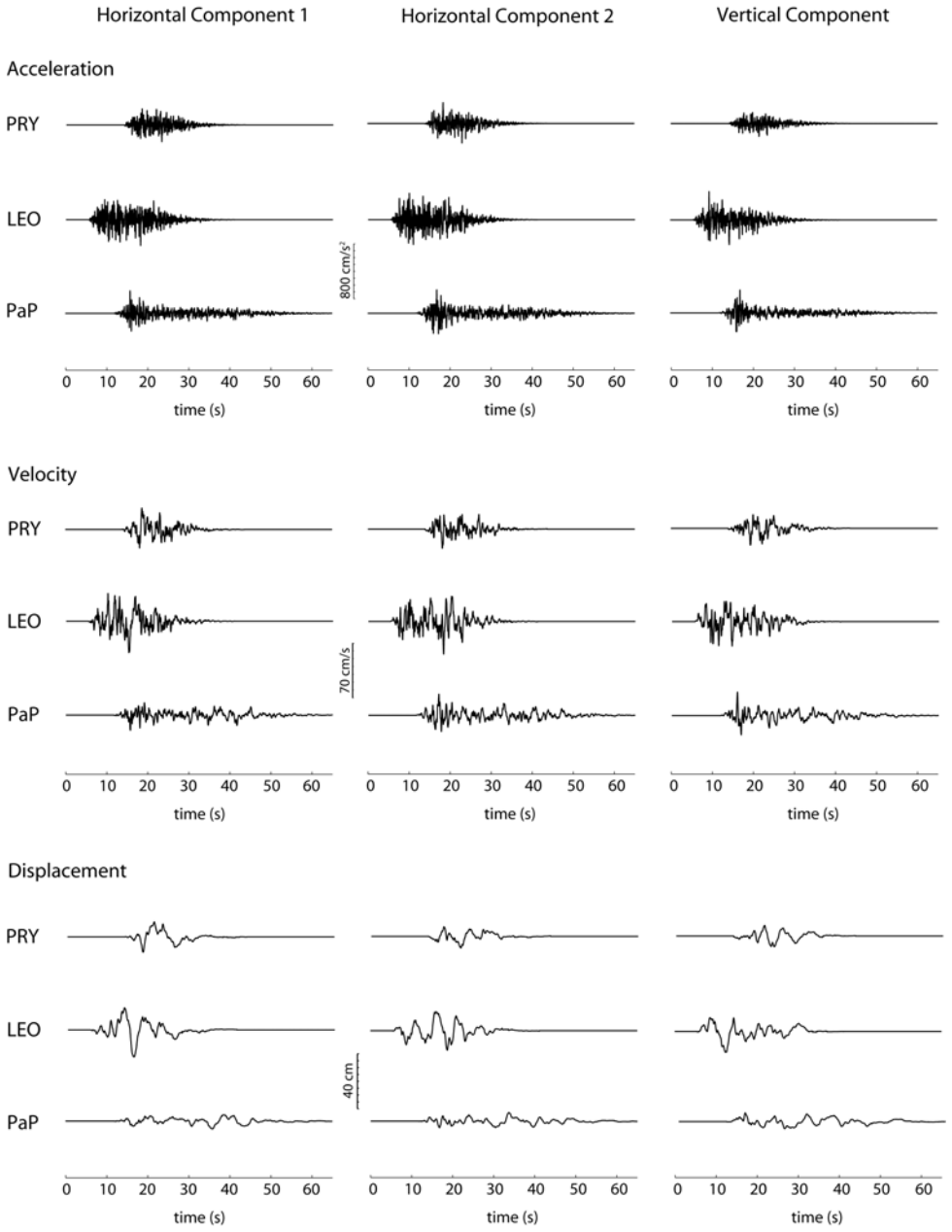

Figure 5. Synthetic high-frequency acceleration, velocity and displacement time histories for selected sites of the 2010 Haiti earthquake. All components are plotted to the same amplitude scale and are uncorrelated.

Figure 5 illustrates time histories of the synthetic high-frequency (f > 0.2 Hz) ground acceleration, velocity and displacement for the cities of Port-au-Prince (PaP), Leogane (LEO) and Port Royal (PRY) over a time window of 65 s. The time series are presented with respect to an absolute time scale whose origin coincides with the nucleation of rupture at the hypocenter on Fault *A*. For all of these sites, the soil category is considered to be National Earthquake Hazards Reduction Program (NEHRP) site class D consistent with the prevailing soil conditions in these locations.

4.3. Broadband ground motion

Figure 6 presents the broadband acceleration, velocity and displacement time histories at Port-au-Prince (PaP), Leogane (LEO) and Port Royal (PRY) obtained by combining the results of low- and high-frequency simulations using matched filtering at a crossover frequency of 1 Hz. The broadband results are presented for three components of acceleration, velocity and displacement. Also shown are the pseudo-acceleration elastic response spectra for a damping ratio of 5%.

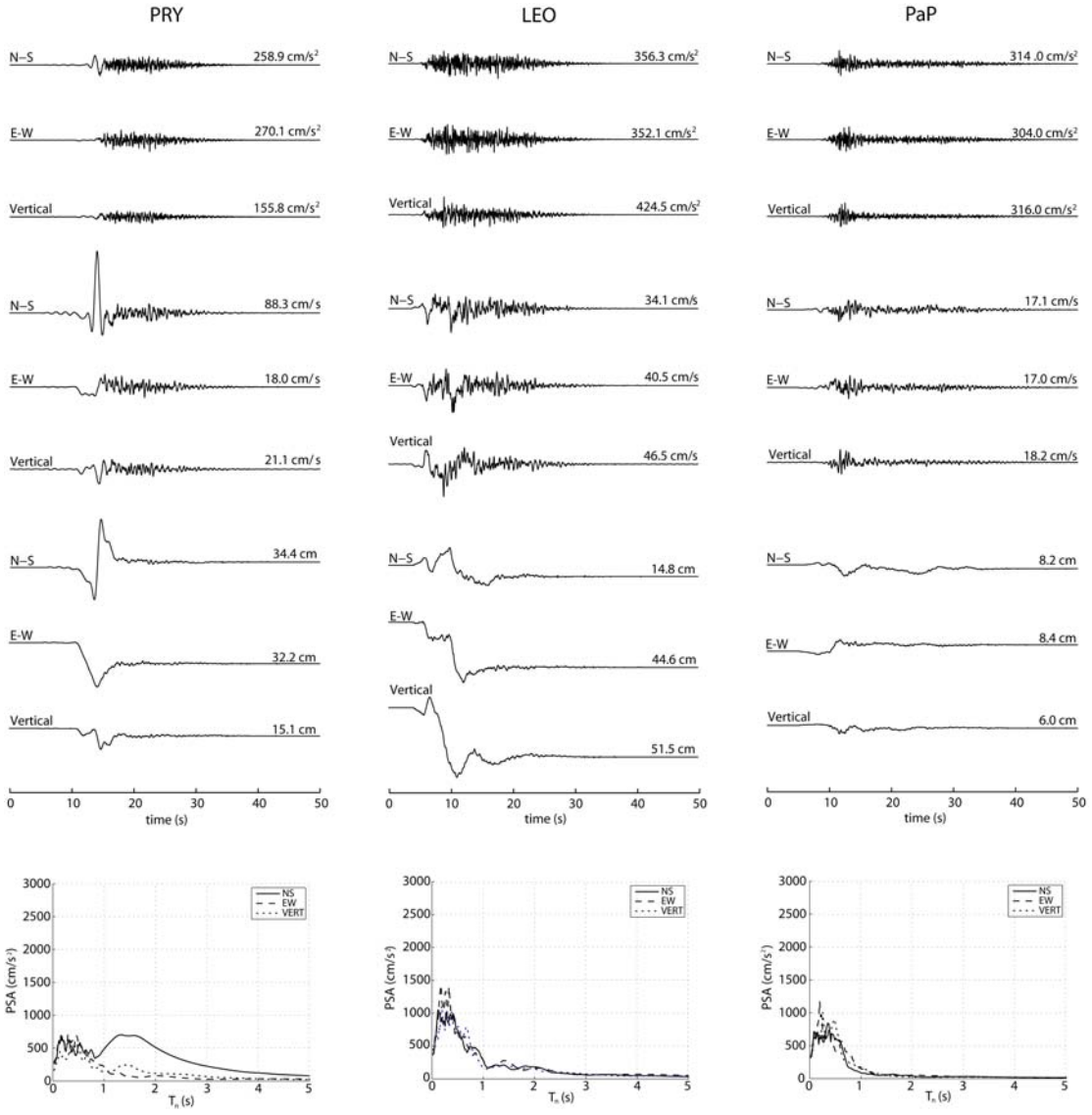

Figure 6. Synthetic broadband acceleration, velocity and displacement time histories and elastic response spectra (5% damping) for selected sites of the 2010 Haiti earthquake.

5. SUMMARY

Although the 2010 M_w 7.0 Haiti earthquake is far from the largest ever recorded, the humanitarian catastrophe and infrastructure damage caused by this seismic event is among the worst in recorded history. This disaster could have been averted had sound design and construction practices been adhered to throughout the affected region. However, Haiti completely lacked a reliable seismic building code to ensure that structures resist ground shaking. In addition, due to the socioeconomic environment, no strong motion instruments were operating in Haiti at the time of the earthquake to record the intensity, duration and frequency content of the ground shaking. In this study, broadband strong ground motions and response spectra were generated for several sites in the vicinity of the 2010 Haiti earthquake, compatible with available seismological observations, geologic field data, and space geodetic measurements. The low-frequency components of the synthetic ground motions were simulated using the discrete wavenumber representation method and the generalized transmission and reflection coefficient technique, while the high-frequency ground motion components were generated using the specific barrier model. The simulation results have the potential to facilitate the development of a relationship between ground motion characteristics and observable damage due to the 2010 earthquake, and therefore contribute to the development of safer seismic design practices in Haiti in the future.

AKCNOWLEDGEMENT

This material is based upon work supported by the National Science Foundation under Grant No. CMMI-1032504. The authors would like to thank Dr. Anthony Sladen for providing the fault slip model of the 2010 Haiti earthquake used in the present study.

REFERENCES

Bouchon, M. (1979). Discrete wave-number representation of elastic wave fields in three-space dimensions, *J. Geophys. Res.* **84**, 3609-3614.

Bouchon, M., and K. Aki (1977). Discrete wave-number representation of seismic-source wave fields, *Bull. Seism. Soc. Am.* **67**, 259-277.

Calais, E., A. Freed, G. Mattioli, F. Amelung, S. Jonsson, P. Jansma, S. H. Hong, T. Dixon, C. Prepetit, and R. Momplaisir (2010). Transpressional rupture of an unmapped fault during the 2010 Haiti earthquake, *Nature Geoscience* **3**, 794–799.

Eberhard, M. O., S. Baldridge, J. Marshall, W. Mooney, and G. J. Rix (2010). The M_w 7.0 Haiti earthquake of January 12, 2010; USGS/EERI Advance Reconnaissance Team report, U.S. Geological Survey Open-File Report 2010-1048.

Halldorsson, B., G. P. Mavroeidis, and A. S. Papageorgiou (2011). Near-fault and far-field strong ground motion simulation for earthquake engineering applications using the specific barrier model, *J. Struct. Eng. – ASCE* **137**, 433-444.

Halldorsson, B., and Papageorgiou, A. S. (2005). Calibration of the specific barrier model to earthquakes of different tectonic regions, *Bull. Seismol. Soc. Am.* **95**, 1276–1300.

Hashimoto, M., Y. Fukushima, and Y. Fukahata (2010). Fan-delta uplift and mountain subsidence during the Haiti 2010 earthquake, *Nature Geoscience* **3**, 255–259.

Hayes, G. P., R. W. Briggs, A. Sladen, E. J. Fielding, C. Prentice, K. Hudnut, P. Mann, F. W. Taylor, A. J. Crone, R. Gold, T. Ito, and M. Simons (2010). Complex rupture during the 12 January 2010 Haiti earthquake, *Nature Geoscience* **3**, 800–805.

Luco, J. E., and R. J. Apsel (1983). On the Green's functions for a layered half-space. Part I, *Bull. Seism. Soc. Am.* **73**, 909-929.

Manaker, D. M., E. Calais, A. M. Freed, S. T. Ali, P. Przybylski, G. Mattioli, P. Jansma, C. Prépetit, and J. B. De Chabalier (2008). Interseismic plate coupling and strain partitioning in the Northeastern Caribbean, *Geophys. J. Int.* **174**, 889–903, doi: 10.1111/j.1365-246X.2008.03819.x

Nettles, M., and V. Hjorleifsdottir (2010). Earthquake source parameters for the 2010 January Haiti main shock and aftershock sequence, *Geophys. J. Int.* **183**, 375-380, doi: 10.1111/j.1365-246X.2010.04732.x

Papageorgiou, A. S. (1988). On two characteristic frequencies of acceleration spectra: Patch corner frequency and f_{max}, *Bull. Seism. Soc. Am.* **78**, 509-529.

Papageorgiou, A. S. (2003). The barrier model and strong ground motion, *Pure Appl. Geophys.* **160**, 603-634.

Papageorgiou, A. S., and K. Aki (1983a). A specific barrier model for the quantitative description of inhomogeneous faulting and the prediction of strong ground motion. I. Description of the model, *Bull. Seism. Soc. Am.* **73**, 693-722.

Papageorgiou, A. S., and K. Aki (1983b). A specific barrier model for the quantitative description of inhomogeneous faulting and the prediction of strong ground motion. II. Applications of the model, *Bull. Seism. Soc. Am.* **73**, 953-978.

Prentice, C. S., P. Mann, A. J. Crone, R. D. Gold, K. W. Hudnut, R. W. Briggs, R. D. Koehler, and P. Jean (2010). Seismic hazard of the Enriquillo-Plantain garden fault in Haiti inferred from palaeoseismology, *Nature Geoscience* **3**, 789-793.

Rathje, E., J. Bachhuber, B. Cox, J. French, R. Green, S. Olson, G. Rix, D. Wells, and O. Suncar (2010). Geotechnical engineering reconnaissance of the 2010 Haiti earthquake, GEER Association Report No. GEER-021.

Wessel, P., and W. H. F. Smith (1991). Free software help map and display data, *Eos Trans. AGU* **72**, 441, doi:10.1029/90EO00319.

Wiggins-Grandison, M. D. (2004). Simultaneous inversion for local earthquake hypocenters, station corrections and 1-D velocity model of the Jamaican crust, *Earth Planet. Sci. Lett.* **224**: 229-240.